International Journal of Scientific Research in Engineering and Management (IJSREM)
Volume: 06 Issue:11 | Nov-2022 SJIF Rating: 7.185 ISSN: 2582-3930

Protection Challenges of Distributed Generation Integration in Radial Distribution Networks: Analysis, Quantification and Mitigation

Nidhi Y. Savjani
Research Scholar, Gujarat Technological University (GTU), India n.savjani1984@gmail.com

***Abstract*—The rapid penetration of distributed generation (DG), particularly rooftop and ground-mounted solar photovoltaic, small hydro, biomass and wind units connected at medium voltage, is transforming passive radial distribution feeders into active networks with bidirectional power flow. Conventional protection schemes, designed on the assumption of unidirectional fault current from a single upstream source, are consequently exposed to a set of well-documented failure modes: protection blinding, sympathetic (false) tripping, recloser–fuse miscoordination, rise in short-circuit level, unintentional islanding and out-of-phase reclosing. This paper presents a structured review of these issues, formulates them analytically using Thévenin equivalent and inverse-time relay models, and quantifies their severity on an 11 kV, 16 km rural radial test feeder with synchronous-machine-based DG (SDG) and inverter-based DG (IBDG) of 0–6 MVA. Results show that a 5 MVA SDG reduces the fault current seen by the substation relay by 21.7%, increases its backup operating time by 36.7%, shrinks its fault-resistance coverage from 15 Ω to 9 Ω, produces a reverse current of 380 A on an adjacent-feeder fault (above the 300 A pickup), and raises the fuse-to-recloser current ratio to 1.72, defeating fuse-saving. Adaptive setting groups with directional supervision and fault current limiters are evaluated as mitigation; the former restores the 0.3 s coordination time interval and extends fault-resistance coverage to 17 Ω. Implications for interconnection practice under IEEE 1547-2018 and Indian CEA connectivity regulations are discussed.**

***Index Terms*—Distributed generation, power system protection, overcurrent relay coordination, protection blinding, sympathetic tripping, recloser–fuse coordination, islanding, inverter-based resources, adaptive protection.**

I. Introduction

Distribution networks have historically been planned as radial systems fed from a single grid substation. Their protection—time-graded overcurrent relays at the substation, line reclosers, sectionalizers and expulsion fuses on laterals—relies on three implicit assumptions: fault current flows in one direction, its magnitude decreases monotonically with electrical distance from the source, and the source impedance is effectively constant [1, 2]. Integration of distributed generation (DG) at medium and low voltage violates all three assumptions.

Policy-driven growth of renewable DG, including feeder-level solar under agricultural solarisation schemes and rooftop programmes in India, means that many 11 kV and 33 kV feeders now host generation comparable in size to their peak load. Early studies by Barker and de Mello [3] and Girgis and Brahma [4] identified the key protection consequences; subsequent work has addressed adaptive protection [5–7], fault current limiters (FCLs) [8], and the distinctive fault behaviour of inverter-based resources [9, 10].

Most reviews describe these issues qualitatively, while numerical studies usually focus on a single phenomenon. The contributions of this paper are: (i) a consolidated taxonomy of DG-related protection problems with their governing mechanisms; (ii) a compact analytical formulation linking DG size and location to relay current, operating time, reach and coordination margin; (iii) a reproducible quantitative case study on a representative rural 11 kV feeder that evaluates five failure modes simultaneously for both SDG and IBDG; and (iv) a comparative assessment of mitigation options against the same metrics.

II. Fault Behaviour of DG Technologies

The protection impact of a DG unit depends primarily on its fault current contribution, which is determined by its interface with the grid (Table I).

Synchronous generators (small hydro, biomass, gas engines) contribute a subtransient current of typically 4–8 pu decaying to a sustained value governed by the excitation system. With directly connected induction generators, contribution is significant only for a few cycles because the machine loses its excitation once terminal voltage collapses [1].

Inverter-based DG (solar PV, battery storage, full-converter wind) contributes current limited by semiconductor ratings, commonly in the range of about 1–2 pu of rated current, with magnitude and phase dictated by the control strategy rather than by physics of the machine [9]. Many inverters inject predominantly balanced positive-sequence current during unbalanced faults, so negative-sequence-based directional and fault-type identification elements may behave unpredictably [10].

III. Protection Issues and Mechanisms

A. Protection Blinding (Under-reach)

When DG is connected between an upstream relay and a downstream fault, it supplies part of the fault current and raises the voltage at its point of connection. The share supplied by the grid through the upstream relay decreases, so the relay operates more slowly or, for high-impedance faults near its reach limit,

TABLE I
FAULT CURRENT CHARACTERISTICS OF DG INTERFACES

DG type	Typical fault contribution	Duration	Main protection concern
Synchronous	4–8 pu (sub-transient)	Sustained	Blinding, fault level rise, miscoordination
Induction	4–6 pu	2–5 cycles	Transient false tripping
Inverter-based	≈1–2 pu, controlled	Control-defined	Low fault signature, sequence-component ambiguity

not at all [4, 11].

B. Sympathetic (False) Tripping

For a fault on an adjacent feeder fed from the same bus, DG on a healthy feeder back-feeds the fault through the healthy feeder's breaker. A non-directional relay may operate on this reverse current, disconnecting healthy load and the DG itself [3].

C. Recloser–Fuse Miscoordination

Feeders commonly use a fuse-saving scheme in which the recloser's fast curve clears temporary faults before the lateral fuse melts. This requires the recloser and fuse currents to be close in magnitude. DG located between the recloser and fuse increases fuse current while reducing recloser current, so the fuse may melt before the recloser's fast operation, converting temporary faults into permanent outages [5, 12].

D. Rise in Short-Circuit Level

DG fault contribution increases the prospective fault level at nearby buses. Existing switchgear, fuses and cable thermal ratings may then be exceeded, and protection settings derived from earlier fault levels lose validity [1].

E. Unintentional Islanding and Out-of-Phase Reclosing

If the upstream breaker opens while DG output closely matches local load, the island may persist undetected. Automatic reclosing onto an unsynchronized island can damage rotating machines and inverters and endanger line crews. IEEE 1547-2018 requires DER to detect an unintentional island and cease to energize within 2 s [13]. Passive methods (under/over-voltage and frequency, rate-of-change-of-frequency, vector shift) have non-detection zones under close power balance; active and communication-based methods reduce these at extra cost [14].

F. Issues Specific to Inverter-Based DG

Low and controlled fault current reduces the margin between load and fault current, complicating overcurrent pickup selection; this is especially critical in islanded microgrids [7, 10]. Distance and directional elements relying on fixed source impedance or negative-sequence quantities may misoperate. Ride-through requirements, which keep DER connected through grid disturbances, may also conflict with fast anti-islanding tripping and must be coordinated [13].

IV. ANALYTICAL FORMULATION

Consider a radial feeder with grid Thévenin impedance Z_S, line impedance Z_1 from the substation to the DG point of connection, Z_2 from the DG to the fault, fault resistance R_f, and DG equivalent impedance Z_{DG}. For a three-phase fault with pre-fault voltage E, the fault current is

$$I_f = \frac{E}{(Z_S + Z_1) \,|\, Z_{DG} + Z_2 + R_f}, \tag{1}$$

and the grid share seen by the substation relay R1 follows from current division:

$$I_{R1} = I_f \frac{Z_{DG}}{Z_S + Z_1 + Z_{DG}}. \tag{2}$$

As DG rating S_{DG} increases, $Z_{DG} \propto 1/S_{DG}$ decreases, so I_f rises while I_{R1} falls: the essence of blinding. The downstream relay R2, beyond the DG, sees the full I_f.

Relays use the IEC standard inverse characteristic [15]

$$t = \mathrm{TMS}\,\frac{0.14}{(I/I_p)^{0.02} - 1}, \tag{3}$$

where I_p is the pickup current. Selectivity requires the coordination time interval

$$\mathrm{CTI} = t_{R1}(I_{R1}) - t_{R2}(I_{R2}) \geq \mathrm{CTI}_{\min}, \tag{4}$$

with $\mathrm{CTI}_{\min} = 0.3$ s for numerical relays. R1's *fault-resistance coverage* as backup is the largest R_f for which $I_{R1} > I_p$. Sympathetic tripping occurs if the reverse current I_{rev} through R1 for an adjacent-feeder fault satisfies $I_{rev} > I_p$ and $t_{R1}(I_{rev})$ is shorter than the clearing time of that feeder's own protection. Fuse-saving requires $k = I_{f\,use}/I_{rec}$ to stay close to unity so that the recloser fast curve operates before the fuse minimum-melt curve over the whole fault range [5].

V. CASE STUDY

A. Test System and Modelling

The test network (Fig. 1) represents a rural 11 kV system. The 11 kV bus has a fault level of 150 MVA with $X/R = 8$. Feeder F1 is 16 km long with four 4 km sections (buses B0–B4), and adjacent feeder F2 is 4 km long (B5 at 2 km, B6 at 4 km). Lines have $0.30 + j0.38\ \Omega$/km. SDG is modelled by $X_d'' = 0.18$ pu plus a step-up transformer of 0.06 pu on its own base. IBDG is modelled as a current source limited to 1.2 pu of rating, in phase quadrature with its terminal voltage. Bolted and resistive three-phase faults are solved by nodal (Z-bus) analysis on a 10 MVA, 11 kV base with 1.0 pu pre-fault voltage, neglecting load. DG of 0–6 MVA is connected at B1 for the relay studies and at B2 for the recloser–fuse study.

Relay R1 (substation, F1) uses $I_p = 300$ A and TMS 0.125; R2 (sectionalizing breaker at B2) uses $I_p = 200$ A and TMS 0.10. These settings achieve CTI ≈ 0.30 s for a fault at B3 without DG. R3 on F2 is set identically to R1. All calculations were scripted in Python and are reproducible from the parameters stated here.

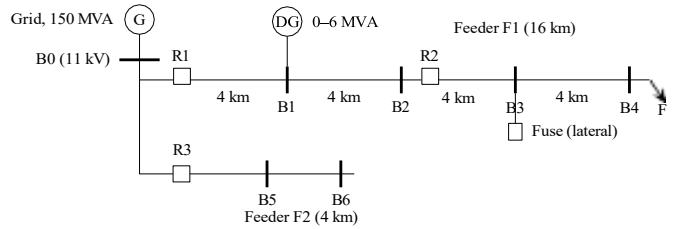


Fig. 1. Single-line diagram of the 11 kV test system. DG is at B1 for relay studies and at B2 for the recloser–fuse study; the lateral fuse is tapped at B3.

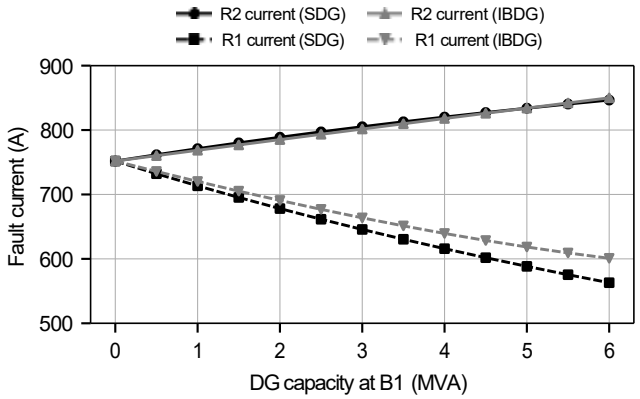


Fig. 2. Fault current through R1 and R2 for a bolted fault at B4 versus DG capacity at B1.

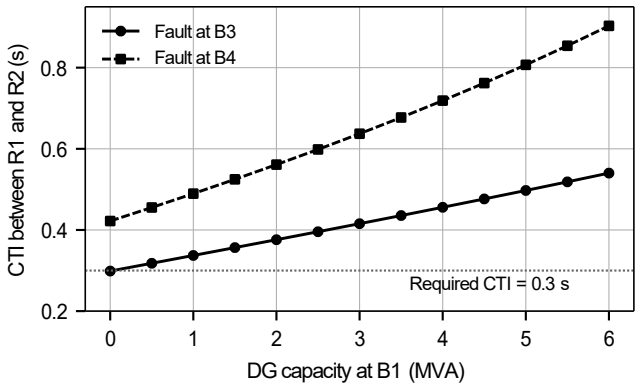


Fig. 3. CTI between R1 and R2 versus SDG capacity at B1.

B. Protection Blinding and Coordination

Fig. 2 shows currents for a bolted fault at the feeder end B4. With 5 MVA SDG, R1 current falls from 752 A to 588 A (−21.7%) while R2 current rises from 752 A to 834 A (+10.9%), consistent with (1)–(2). IBDG of the same rating reduces R1 current to 618 A (−17.8%): smaller, but not negligible, because even limited injection raises the voltage at B1.

Because R2 is accelerated and R1 decelerated, the CTI widens rather than collapsing (Fig. 3): at B4 it grows from 0.42 s to 0.81 s at 5 MVA. Selectivity is therefore retained, but R1 backup clearing time increases from 0.94 s to 1.29 s (+36.7%), raising let-through energy and equipment stress if R2 fails. The time–current curves in Fig. 6 illustrate the shift of operating points.

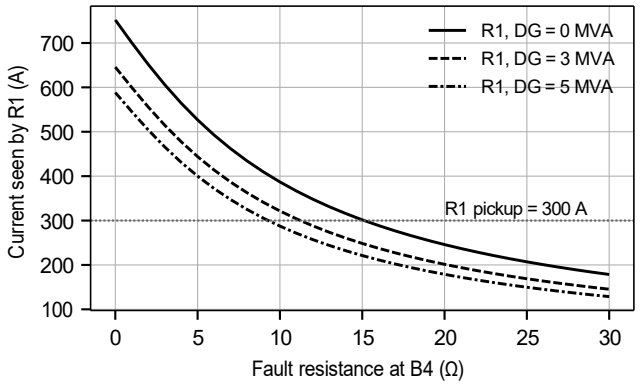


Fig. 4. Current seen by R1 for a resistive fault at B4 versus fault resistance.

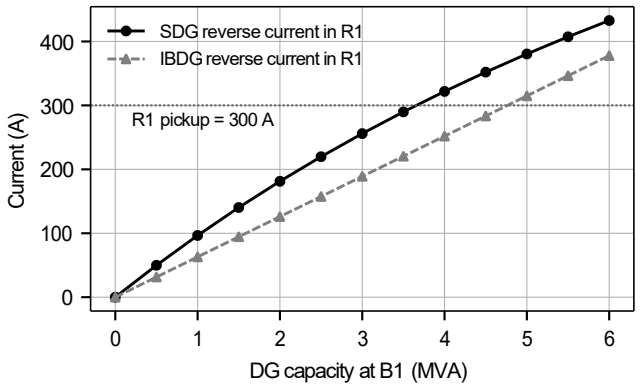


Fig. 5. Reverse current through R1 for a fault at B5 on adjacent feeder F2.

The more serious consequence appears for resistive faults (Fig. 4). Without DG, R1 detects faults at B4 up to R_f = 15 Ω; with 3 MVA and 5 MVA SDG this coverage shrinks to 11 Ω and 9 Ω, respectively. For faults between 9 and 15 Ω, R1 provides no backup at all with 5 MVA DG, which is true blinding.

C. Sympathetic Tripping

For a bolted fault at B5 on F2, DG on F1 back-feeds through R1 (Fig. 5). The reverse current exceeds R1's 300 A pickup once SDG exceeds 3.7 MVA (4.8 MVA for IBDG), reaching 380 A at 5 MVA. With the inverse-time setting, R1 would operate in 3.67 s, whereas R3 clears the 3.88 kA fault in 0.33 s, so R1 resets in this case. However, any instantaneous or definite-time element on R1 set below 380 A, a slower F2 device, or a failed R3 would cause healthy feeder F1 to trip. The margin is thus a function of DG size and is not guaranteed by design.

D. Influence of DG Location

Table II repeats the bolted and resistive fault analysis for a fault at B4 with a 5 MVA SDG placed at B1, B2 and B3. Two observations follow. First, the reverse current that drives sympathetic tripping is largest for DG close to the substation (380 A at B1) and falls with distance (262 A at B3) because the line impedance between DG and bus limits the back-feed. Second, R1 coverage degrades further as DG moves downstream (9 Ω to 7 Ω). When DG is located beyond R2 (at B3), R2 itself is

TABLE II
EFFECT OF DG LOCATION (5 MVA SDG, FAULT AT B4)

Metric	DG at B1	DG at B2	DG at B3
I_{R1} (A) / t_{R1} (s)	588 / 1.29	574 / 1.34	619 / 1.20
I_{R2} (A) / t_{R2} (s)	834 / 0.48	985 / 0.43	619 / 0.61
R1 coverage R_f (Ω)	9.0	7.5	7.0
Reverse current, fault at B5 (A)	380	311	262

TABLE III
SUMMARY OF CASE-STUDY RESULTS

Metric (SDG at B1 unless noted)	0 MVA	3 MVA	5 MVA
I_{R1}, fault at B4 (A)	752	646	588
I_{R2}, fault at B4 (A)	752	805	834
t_{R1} backup, fault at B4 (s)	0.944	1.133	1.290
CTI, fault at B3 (s)	0.299	0.416	0.497
R1 fault-resistance coverage (Ω)	15	11	9
Reverse current in R1, fault at B5 (A)	0	256	380
Fault level at B1 (MVA)	45.5	56.7	64.5
$k = I_{fuse}/I_{rec}$ (DG at B2)	1.00	1.42	1.72

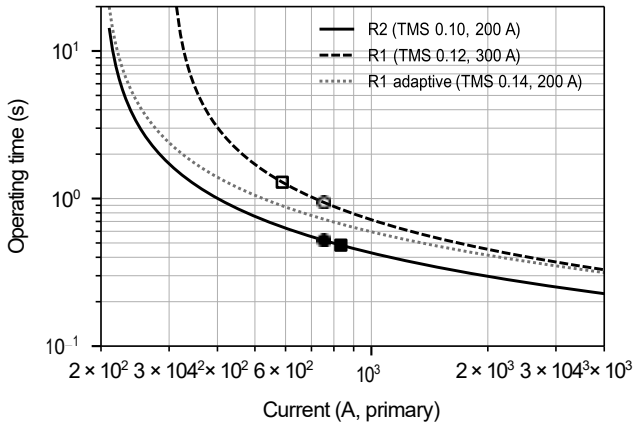


Fig. 6. Time–current characteristics of R1, R2 and the adaptive R1 setting. Filled markers: R2; hollow markers: R1 (circles: no DG; squares: 5 MVA DG) for a fault at B4.

blinded: its current falls from 752 A (no DG) to 619 A and its operating time rises from 0.52 s to 0.61 s. Hence blinding affects whichever device lies upstream of the DG, and siting rules must consider every protective device on the path, not only the substation breaker.

E. Recloser–Fuse Coordination and Fault Level

With DG at B2 and a fault on the lateral at B3, the fuse-to-recloser current ratio k rises from 1.00 to 1.42 at 3 MVA and 1.72 at 5 MVA (Table III). At 5 MVA, fuse current increases by 43.5% while recloser current decreases by 16.4%, so the recloser fast curve can no longer be guaranteed to operate before fuse melting over the upper fault-current range. Fault level at B1 rises from 45.5 MVA to 64.5 MVA (+41.8%) and at the 11 kV bus from 150 MVA to 166.3 MVA (+10.9%). This remains within typical 11 kV switchgear ratings here, but cumulative DG on several feeders can erode margins at stiffer substations.

TABLE IV
MITIGATION PERFORMANCE AT 5 MVA SDG

Metric	None	Adaptive + dir.	FCL 0.5 pu
t_{R1}, fault at B4 (s)	1.290	0.892	1.094
CTI, fault at B3 (s)	0.497	0.300	0.394
Coverage R_f (Ω)	9	17	11.5
Reverse trip risk, fault at B5	Yes (380 A)	Blocked	No (216 A)

VI. MITIGATION TECHNIQUES

A. Review of Approaches

Directional overcurrent relays at feeder heads block reverse operation and remove the sympathetic-tripping risk, but require voltage transformers and careful polarization for IBDG [8]. *Adaptive protection* switches relay setting groups according to DG status, measured by breaker status or communications, so that pickup and TMS track the network state [5–7]. *Fault current limiters* in series with DG restrict its contribution during faults while remaining nearly transparent in normal operation [8]. *Penetration limits and siting rules* cap DG size where protection cannot be adapted. *Communication-assisted schemes* (permissive/blocking, line differential, transfer trip) provide selectivity independent of current magnitude and support anti-islanding [10]. *Voltage-based and sequence-component elements* supplement overcurrent detection where IBDG fault currents are low [16].

B. Evaluation on the Test Feeder

Two options were evaluated at 5 MVA SDG (Table IV). An adaptive setting group for R1 (I_p = 200 A, TMS 0.139, activated when DG is connected) with directional supervision restores CTI to exactly 0.30 s at B3, reduces R1 backup time at B4 to 0.89 s (below the no-DG value) and extends fault-resistance coverage to 17 Ω; the directional element blocks reverse operation. The lower pickup must remain above the feeder's maximum load current with a suitable margin, which should be verified for each feeder. An FCL of 0.5 pu (on 10 MVA base) at the DG terminal partially relieves blinding (coverage 11.5 Ω, t_{R1} = 1.09 s) and reduces reverse current to 216 A, below pickup, without relay changes. It does not, however, restore the original coordination as fully as adaptive settings.

VII. DISCUSSION AND REGULATORY CONTEXT

The results indicate that the most consequential issue for medium-sized SDG on long rural feeders is loss of backup coverage for resistive faults, not loss of selectivity. Blinding increases with feeder length, weaker source fault level and DG proximity to the substation relay, so rural feeders typical of agricultural networks are most exposed. For IBDG, magnitude effects are smaller, but the low and control-dependent fault signature shifts the challenge toward detection and directional discrimination, particularly where the feeder can operate as an island.

IEEE 1547-2018 [13] specifies response to abnormal voltage and frequency, ride-through categories, unintentional-islanding detection within 2 s, and coordination with utility reclosing. In India, the CEA (Technical Standards for Connectivity of

the Distributed Generation Resources) Regulations, 2013, as amended in 2019 [17], require DG to provide anti-islanding protection and comply with prescribed protection and power-quality requirements. Neither framework, however, prescribes feeder-level protection re-studies as DG accumulates. Utility practice can address these gaps through a staged approach. At low penetration, a protection review limited to pickup margins and fault level is generally adequate. At moderate penetration, directional elements at feeder heads, revised recloser fast-curve settings and verification of fuse-saving ranges become necessary. At high penetration or where feeders may be islanded, adaptive or communication-assisted protection, transfer trip to DG on breaker opening, and supervised (voltage-checked) reclosing should be adopted. Numerical relays with multiple setting groups, already common in new substations, make the adaptive option inexpensive to implement once DG status signals are available through SCADA or distribution automation.

A practical recommendation is to make a protection impact assessment, covering the metrics in Table III, a mandatory part of the interconnection study whenever cumulative DG on a feeder exceeds a defined fraction of its peak load or of its minimum fault level.

VIII. Conclusion

This paper reviewed and quantified the protection issues caused by DG integration in radial distribution systems. On a representative 11 kV, 16 km feeder, 5 MVA of synchronous DG reduced substation relay current by 21.7%, increased backup time by 36.7%, reduced fault-resistance coverage from 15 Ω to 9 Ω, created a reverse current above relay pickup for adjacent-feeder faults, and raised the fuse-to-recloser current ratio to 1.72, defeating fuse-saving. Inverter-based DG produced smaller magnitude effects but introduced detection and discrimination difficulties. Adaptive setting groups with directional supervision gave the most complete restoration of protection performance, while FCLs offered a relay-independent partial remedy. Future work will extend the analysis to unbalanced faults with grid-code-compliant IBDG control, time-domain validation, and communication-based adaptive schemes for feeders with high DG penetration.

References

[1] N. Jenkins, R. Allan, P. Crossley, D. Kirschen, and G. Strbac, *Embedded Generation*. London, U.K.: IET, 2000.

[2] *IEEE Recommended Practice for Protection and Coordination of Industrial and Commercial Power Systems (IEEE Buff Book)*, IEEE Std 242-2001, 2001.

[3] P. P. Barker and R. W. de Mello, "Determining the impact of distributed generation on power systems. I. Radial distribution systems," in *Proc. IEEE PES Summer Meeting*, Seattle, WA, USA, 2000, vol. 3, pp. 1645–1656.

[4] A. Girgis and S. Brahma, "Effect of distributed generation on protective device coordination in distribution system," in *Proc. Large Engineering Systems Conf. Power Engineering (LESCOPE)*, Halifax, NS, Canada, 2001, pp. 115–119.

[5] S. M. Brahma and A. A. Girgis, "Development of adaptive protection scheme for distribution systems with high penetration of distributed generation," *IEEE Trans. Power Del.*, vol. 19, no. 1, pp. 56–63, Jan. 2004.

[6] P. Mahat, Z. Chen, B. Bak-Jensen, and C. L. Bak, "A simple adaptive overcurrent protection of distribution systems with distributed generation," *IEEE Trans. Smart Grid*, vol. 2, no. 3, pp. 428–437, Sep. 2011.

[7] A. Oudalov and A. Fidigatti, "Adaptive network protection in microgrids," *Int. J. Distrib. Energy Resour.*, vol. 5, no. 3, pp. 201–226, 2009.

[8] W. El-Khattam and T. S. Sidhu, "Restoration of directional overcurrent relay coordination in distributed generation systems utilizing fault current limiter," *IEEE Trans. Power Del.*, vol. 23, no. 2, pp. 576–585, Apr. 2008.

[9] J. Keller and B. Kroposki, "Understanding fault characteristics of inverter-based distributed energy resources," National Renewable Energy Laboratory, Golden, CO, USA, Tech. Rep. NREL/TP-550-46698, Jan. 2010.

[10] A. Hooshyar and R. Iravani, "Microgrid protection," *Proc. IEEE*, vol. 105, no. 7, pp. 1332–1353, Jul. 2017.

[11] N. Hadjsaid, J.-F. Canard, and F. Dumas, "Dispersed generation impact on distribution networks," *IEEE Comput. Appl. Power*, vol. 12, no. 2, pp. 22–28, Apr. 1999.

[12] H. B. Funmilayo and K. L. Butler-Purry, "An approach to mitigate the impact of distributed generation on the overcurrent protection scheme for radial feeders," in *Proc. IEEE/PES Power Systems Conf. Expo. (PSCE)*, Seattle, WA, USA, 2009, pp. 1–11.

[13] *IEEE Standard for Interconnection and Interoperability of Distributed Energy Resources with Associated Electric Power Systems Interfaces*, IEEE Std 1547-2018, 2018.

[14] H. Zeineldin, E. F. El-Saadany, and M. M. A. Salama, "Distributed generation micro-grid operation: Control and protection," in *Proc. Power Systems Conf.: Advanced Metering, Protection, Control, Communication, and Distributed Resources*, Clemson, SC, USA, 2006, pp. 105–111.

[15] *Measuring Relays and Protection Equipment—Part 151: Functional Requirements for Over/Under Current Protection*, IEC 60255-151, 2009.

[16] J. C. Gómez and M. M. Morcos, "Coordination of voltage sag and overcurrent protection in DG systems," *IEEE Trans. Power Del.*, vol. 20, no. 1, pp. 214–218, Jan. 2005.

[17] Central Electricity Authority, *Central Electricity Authority (Technical Standards for Connectivity of the Distributed Generation Resources) Regulations, 2013*, Gazette of India, New Delhi, India, 2013 (amended 2019).